Letter

Orthogonality catastrophe beyond bosonization from post-selection

Martino Stefanini * and Jamir Marino
Institut für Physik, Johannes Gutenberg-Universität Mainz, D-55099 Mainz, Germany

(Received 27 October 2023; revised 12 June 2024; accepted 13 August 2024; published 23 October 2024)

We show that the dynamics induced by post-selected measurements can serve as a controlled route to access physical processes beyond the boundaries of Luttinger liquid physics. We consider a one-dimensional fermionic wire whose dynamics results from a sequence of weak measurements of the fermionic density at a given site, interspersed with unitary hopping dynamics. This realizes a non-Hermitian variant of the celebrated instance of a local scatterer in a fermionic system and its ensuing orthogonality catastrophe. We observe a distinct crossover in the system's time evolution as a function of the fermion density. In the high-density regime, reminiscent of the Hermitian case, a bosonized version of the model properly describes the dynamics while, as we delve into the low-density regime, the validity of bosonization breaks down, giving rise to irreversible behavior. Notably, this crossover from reversible to irreversible dynamics is nonperturbative in the measurement rate and can manifest itself even with relatively shallow measurement rates, provided that the system's density remains below the crossover threshold. Our results render a conceptually transparent model for exploring nonperturbative effects beyond bosonization, which could be used as a stepping stone to explore novel routes for the control of nonlinear dynamics in low-dimensional quantum systems.

DOI: 10.1103/PhysRevResearch.6.L042022

Introduction. The Tomonaga-Luttinger liquid (TLL) stands as the universal, low-energy description for interacting one-dimensional (1D) quantum systems, renowned for its mathematical elegance and success in equilibrium scenarios [1,2]. Its technical cornerstone, known as bosonization, allows to transform virtually any interacting system involving 1D fermions, bosons, or spins into a massless free theory of collective bosonic excitations. Extending its applicability beyond equilibrium, especially in nonequilibrium settings, has been a topic of exploration in both isolated [3–11] and open systems [12–16], as well as in the realm of non-Hermitian systems [17–24] and measurement-induced dynamics [25–29].

While the TLL framework proves remarkably robust even far from equilibrium in certain phenomenological cases [9,14,30–33], it lacks a formal renormalization group argument to guarantee its validity given the potential excitation of higher-energy degrees of freedom. The exploration of dynamics beyond TLL at equilibrium has seen significant attention in recent decades [34], yet understanding its validity in nonequilibrium conditions remains largely uncharted territory. This is partly due to the inherent technical challenges posed by the problem itself [35–37] and the absence of iconic models to guide such inquiries.

Nonetheless, delving into this line of inquiry holds both fundamental and practical significance. It serves as a potential testing ground for theories encompassing universal dynamics beyond traditional thermodynamics, while also offering the prospect of discovering effective models capable of simplifying the numerical resolution of highly correlated quantum dynamics.

In this Letter, we embark on an initial exploration in this direction by proposing a model of nonunitary dynamics where nonperturbative effects beyond bosonization manifest in a controlled fashion, and where at the same time the mechanisms for the breakdown of bosonization can be traced back to a transparent physical picture. The latter feature is highly nontrivial, since there are only a few cases [34,36] in which the breakdown is physically well understood. We implement a non-Hermitian version of the orthogonality catastrophe (OC) using post-selected continuous measurements of the local fermionic density at a given site. The OC [1,2,38,39] is a paradigmatic phenomenon in solid-state physics, with countless applications ranging from the physics of x-rays [39,40] to the Kondo effect [41–43], quantum dots [44,45], and ultracold atoms [46–48]. The OC describes the strong sensitivity of gapless fermionic systems to local perturbations: a single scattering center introduced in a metal generates a new ground state which is orthogonal to the unperturbed one [38], due to the excitation of a diverging number of particle-hole pairs with vanishing energy. The dynamical signature of the OC is an algebraic decay in time of the return amplitude after turning on of the local potential. This characteristic decay has been proven by nonperturbative means [49,50], but it is also predicted by a simple bosonized description [40]—an early example of a successful nonequilibrium application of bosonization.

In this study, we consider a model where a local imaginary scattering potential is abruptly introduced into a

*Contact author: mstefa@uni-mainz.de

noninteracting 1D fermionic system. While nonequilibrium versions of the OC problem have been explored in previous literature [51–54], our approach is distinct. We employ post-selection of measurements, which plays a pivotal role in our ability to control the extent to which the dynamics deviate from an effective bosonized description. Our primary focus is on the return amplitude $\mathcal{L}(t) \equiv \langle\psi(0)|\psi(t)\rangle$, which serves as a global indicator of how closely the full state aligns with the description provided by bosonization. Our findings reveal a distinct algebraic decay in $\mathcal{L}(t)$, consistent with the Hermitian scenario. However, in the non-Hermitian setting, we observe an additional exponential decay not anticipated by bosonization. Unlike conventional occurrences of decoherence in OC [51–53], this exponential decay signifies a reversible/irreversible dynamical crossover directly associated with the breakdown of bosonization. This feature stands as a unique hallmark of our post-selected implementation of the OC. The presence of a decay rate, indicative of irreversible dynamics, strongly depends on the initial density of fermions: it is significant only in the low-density regime, where deviations from bosonization are notable, but tapers to zero as the background fermion density increases. This perspective is corroborated by our examination of the system's kinetic energy, which grows linearly over time. This growth hints at the existence of energy absorption processes that naturally drive deviations from the bosonization description whenever fermionic densities are low.

We interpret the breakdown of bosonization at low densities as a consequence of the presence of quasibound states in the single-particle spectrum of the non-Hermitian Hamiltonian that governs the dynamics. These states occur far from the Fermi surface, and exert their influence through the imaginary part of their eigenvalues. They exist because of the curvature of the fermionic dispersion, and so they disappear as the dispersion is linearized when bosonizing the Hamiltonian.

Model. We consider a 1D system of noninteracting, spinless fermions c_j that can hop on the lattice sites of a chain according to the Hamiltonian $H = -J\sum_{j=0}^{L-1}(c_{j+1}^\dagger c_j + c_j^\dagger c_{j+1}) = \sum_q \varepsilon_q c_q^\dagger c_q$. The chain has L sites with periodic boundary conditions (pbc) and unit lattice spacing $a = 1$. We also use units such that $\hbar = 1$. The momentum modes are $c_q = L^{-1/2}\sum_j \mathrm{e}^{-\mathrm{i}qj}c_j$, corresponding to energies $\varepsilon_q \equiv -2J\cos q$.

We assume that the system is initialized in its ground state $|FS\rangle$ (at a certain filling N_f, namely density $\bar{n} = N_f/L$), and then evolves according to the nonlinear Schrödinger equation

$$\mathrm{i}\frac{d}{dt}|\psi(t)\rangle = \left[K + \mathrm{i}\frac{\gamma}{2}\langle\psi(t)|\, n_0\, |\psi(t)\rangle\right]|\psi(t)\rangle\,, \qquad (1)$$

where γ is a constant that can be of either sign, $n_0 \equiv c_{j_0}^\dagger c_{j_0}$ is the number operator at the site j_0, and where we have introduced the non-Hermitian Hamiltonian

$$K \equiv H - \mathrm{i}\frac{\gamma}{2}n_0. \qquad (2)$$

The above Hamiltonian [15,55–57] describes scattering off a localized potential (i.e., an impurity) that has an imaginary strength. It can be seen as the simplest non-Hermitian generalization of the OC problem. Equation (1) can be solved as $|\psi(t)\rangle = |\tilde{\psi}(t)\rangle/\langle\tilde{\psi}(t)|\tilde{\psi}(t)\rangle^{1/2}$, where $|\tilde{\psi}(t)\rangle = \mathrm{e}^{-\mathrm{i}Kt}|\psi(0)\rangle$, so that the dynamics is simply the normalized version of the nonunitary evolution generated by K.

There are several scenarios that lead to the dynamics (1), and all of them have in common some form of post-selection. We briefly present here a few of the simplest strategies, leaving a more detailed discussion to the Supplemental Material [58].

The most conceptually straightforward scenario is that of continuous monitoring [59,60]: the system undergoes a series of weak measurements of the density at site j_0 at a rate γ, interspersed with Hamiltonian evolution, with a set of measurement operators that includes

$$M(\delta t) = \mathcal{N}\mathrm{e}^{-\frac{\gamma\delta t}{2}n_0}, \qquad (3)$$

along with other operators that we do not need to specify here ($\mathcal{N}$ is a suitable normalization constant that plays no role). Such dynamics would yield stochastic state trajectories, conditioned on the random measurement outcomes, and (1) is obtained by selecting only those trajectories in which the outcome is always the one corresponding to the action of (3). This procedure is known as the no-click limit [25,61–63]. Physically, the measurement operator (3) for $\gamma > 0$ may be taken to represent a measurement that has found no particles at j_0, since it favors states with $n_0 = 0$. Vice versa, $\gamma < 0$ represents a measurement that finds one particle at j_0.

It is also possible to simulate (1) with a dissipative dynamics governed by a Lindblad master equation, if the jump operator $\mathcal{J}$ [59,64] is such that the non-Hermitian part of the dissipative dynamics $\widetilde{H} = H - \frac{\mathrm{i}}{2}\mathcal{J}^\dagger\mathcal{J}$ reproduces (2) [65] and if the dynamics can be confined to a suitable subspace by a post-selection of experimental runs [18,66,67]. A simple example is provided by a localized single particle loss $\mathcal{J} = \gamma^{1/2}c_{j_0}$ [15,68–70]. For each time t of the dynamics, the total number of particles is measured and only the runs in which no fermions have been lost are kept. The observables measured within this set of runs correspond to the state $|\tilde{\psi}(t)\rangle$, and must be divided by its squared norm, which is simply the probability of not losing particles in the time t. This form of post-selection can be extended to any dissipative dynamics for which there is a way to recognize the effect of dissipative events, the so-called jumps [64]. For instance, this procedure is possible for localized single particle gain $\mathcal{J} = \gamma_g^{1/2}c_{j_0}^\dagger$ [71], which corresponds to $\gamma = -\gamma_g < 0$, while it is not viable for localized dephasing $\mathcal{J} = \gamma^{1/2}n_0$ [51,72]. It should be possible to implement the procedure above in near-term experiments (e.g., see [67,73]) for localized losses [74–78]. The two strategies outlined above (measurement and dissipation based) are closely related, but while the first requires monitoring a local observable at each instant of time, the second only requires global measurements at the end of the dynamics.

A different dissipative strategy employs an immobile impurity particle that induces a localized two-body loss [79–84] in the system, i.e., $\mathcal{J} = \gamma^{1/2}d\,c_{j_0}$, where d annihilates the impurity. Then, the effective Hamiltonian $\widetilde{H} = H - \mathrm{i}\gamma/2\, n_0\, d^\dagger d$ can be switched from H to K by simply injecting the impurity, $d^\dagger d = 1$. Finally, in analogy with the Hermitian scenario [47,85], one only needs to measure observables of the impurity to reconstruct the dynamics (1). This strategy does not require post-selection of the experimental runs.

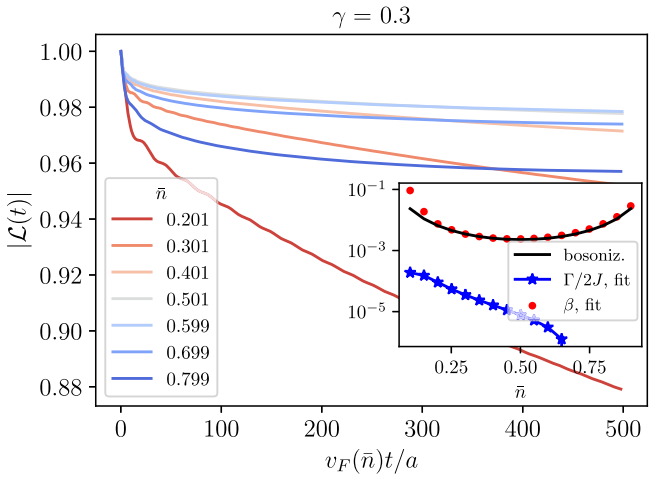

FIG. 1. Absolute value of the return amplitude as a function of the rescaled time for $L = 1000$, $J = 0.5$, $\gamma = 0.3$, and increasing density. The plot shows the absence of particle-hole symmetry as the low-density curves (in shades of red) decay faster than those at the conjugate densities $1 - \bar{n}$ (shades of blue) because of an additional exponential envelope caused by the post-selected measurements. Inset: filling dependence of the two fitting parameters β (OC exponent, red dots) and Γ (exponential decay rate, blue stars), along with the bosonization prediction for β (black line). The uncertainty on the fitted parameters is smaller than the size of the marker points.

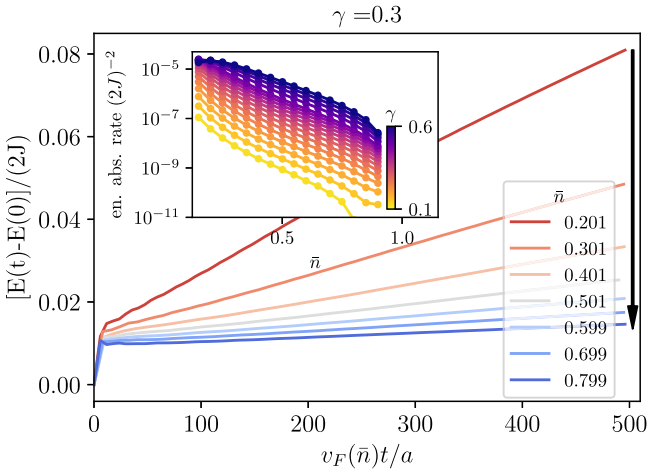

FIG. 2. Energy absorption as a function of the rescaled time for $L = 1000$, $J = 0.5$, $\gamma = 0.3$, and various densities. A monotonic behavior as a function of the density can be observed in the rate of energy absorption after a transient, which decreases upon increasing the density, as emphasized by the arrow on the right of the figure. Inset: density dependence of the energy absorption rate computed from a linear fit, at various values of γ. The rate decays exponentially with $\bar{n}$.

Numerical evidences. We have computed the time evolution of the system using the algorithm described in Ref. [86]: we evolve the matrix of the single-particle wavefunctions $U_{ji} = [\phi_{p_i}(j)]_{j=1,\dots,L}^{i=1,\dots,N_f}$ with the single-particle versions of H and M, and we keep the state normalized at each step.

We focus here on two main observables: the return amplitude and the total energy. The return amplitude is defined as $\mathcal{L}(t) \equiv \langle\psi(0)\,|\psi(t)\rangle = \langle FS\,|\psi(t)\rangle$, which is variously known as fidelity, Loschmidt echo, or impurity Green's function. As stated in the introduction, a power-law decay of the return amplitude is the hallmark of the OC [1,2,39].

The typical behavior of the return amplitude is shown in Fig. 1. Our numerical computations show that after an initial transient, $|\mathcal{L}(t)|$ displays two qualitatively different behaviors, and that we can go from one to the other by tuning the density. Above half filling, the return amplitude is well described by a power law, while below it acquires an exponential decay. Notice that the lack of symmetry with respect to half-filling is to be expected, as the dynamics (1) explicitly breaks particle-hole symmetry: loosely speaking, the exchange $c_j \leftrightarrow (-1)^j c_j^\dagger$ leaves the Hamiltonian invariant while changing the sign of γ [58]. As a consequence, we will show only data for $\gamma > 0$, as those for $\gamma < 0$ (for the case of post-selection for $n_0 = 1$) can be obtained from the correspondence $\bar{n}(\gamma < 0)$=1−$\bar{n}(\gamma > 0)$.

We fit $|\mathcal{L}(t)|$ assuming that after the transient it has the form $|\mathcal{L}(t)| = At^{-\beta}\mathrm{e}^{-\Gamma t}$. The combined algebraic and exponential decay reflects the two processes that we expect to occur: the former is the OC behavior, while we interpret the latter as a sign of irreversible dynamics caused by the measurement process. This shape of $|\mathcal{L}(t)|$ is valid for $0.1 \lesssim \bar{n} \lesssim 0.9$ and $\gamma \lesssim J$: outside this range of parameters, the return amplitude has a more complicated behavior.

The typical density dependence of the two parameters β (the OC exponent) and Γ (the decay rate) for a chain of $L = 1000$ sites is shown in the inset of Fig. 1. The two parameters behave very differently: while β is essentially particle-hole symmetric, Γ decreases monotonically (and exponentially) with the filling. We show in [58] that the behavior of the OC exponent β can be predicted with bosonization, which yields $\beta_b(\bar{n}) = \gamma^2/[2\pi v_F(\bar{n})]^2$. This expression depends on the filling only through the Fermi velocity $v_F = 2J\sin(\pi\bar{n})$, which is particle-hole symmetric, in accord with the numerics [87]. However, the power-law behavior is all that bosonization predicts. Namely, the existence of a nonvanishing Γ lies beyond bosonization. A numerical fit indicates (cf. [58]) that for small γ the decay rate behaves as $\ln\Gamma \approx a(\gamma) - b\bar{n}/\gamma^y$, where $a(\gamma)$ is approximately linear in γ, $b > 0$, and $y \approx 1.4$. This result suggests that Γ is nonperturbative in the measurement rate γ.

A second observable that we consider is the kinetic energy absorbed as a function of time, $E(t) \equiv \langle\psi(t)|\,H\,|\psi(t)\rangle$, whose evolution is shown in Fig. 2 for a fixed γ at various fillings. This quantity shows a steep transient, after which it begins to grow linearly in time. The interesting behavior is the dependence of the slope of the linear growth (namely, the energy absorption rate) on the filling. The inset in Fig. 2 shows that the rate decreases exponentially with the fermion density. In the case of our model, bosonization would predict that the energy should saturate as a function of time, as in the Hermitian case. This predicted behavior depends on the excitation of only low-energy modes, which are those captured by the TLL Hamiltonian. The absorption of energy in the non-Hermitian scenario signals the broken time-reversal symmetry—or irreversibility—of the dynamics of the measured system. Indeed, the state will eventually converge to the many-body eigenstate of K with the smallest imaginary part of the eigenvalue, although this happens at very late times [15,72], much larger than L/v_F.

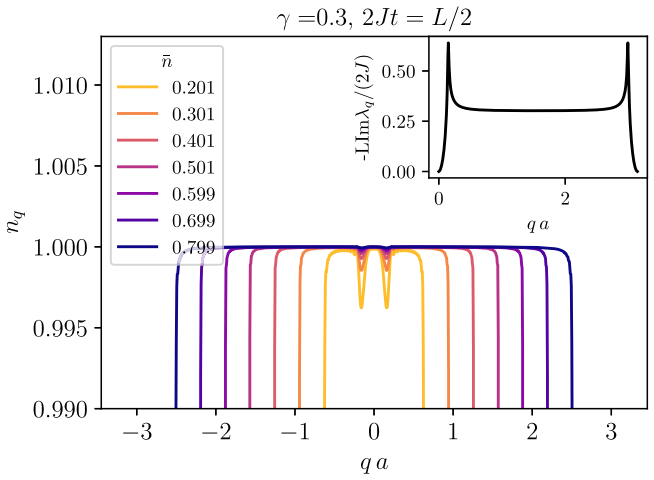

FIG. 3. Occupation of the momentum states in the Brillouin zone for a system of $L = 1000$ sites at the time $2Jt = L/2$, with $2J = 1$ and the measurement rate fixed at $\gamma/2J = 0.3$. The plot reveals the extra depletion around the modes $q^* \approx \pm \arcsin \gamma/4J$, which cannot be accounted for by bosonization, and it shows how the depletion is deeper for smaller initial filling. The inset reports the imaginary part of the single-particle eigenvalues of the non-Hermitian Hamiltonian (2), displaying that the depleted modes correspond to a peak of the single-particle decay rates.

We would like to point out that the value of the measurement rate γ does not play an important role in our results, as in all the plots that we are showing it is smaller than the bandwidth $4J$. In this parameter regime, a larger γ determines a quantitative change of the various effects, while the qualitative picture remains unchanged [88]. In the Hermitian OC scenario, the smallness of the impurity potential ensures the applicability of bosonization, but the power-law behavior is nonperturbative [1,2,49,50]. Our calculations show that for the non-Hermitian version of the OC, bosonization is not applicable—yielding qualitatively wrong predictions—even in such perturbative regime.

Physical mechanism. As observed in the numerics, the predictions of bosonization are violated if the density is low enough. We stress that our TLL predictions involve no approximations beyond the linearization of the dispersion relation, since we bosonize the model in such a way [1,2,89] that a quadratic Hamiltonian is obtained, to which no nonlinear terms need to be added within the usual theory of TLL. The validity of the linearization of the spectrum around the Fermi points typically relies only on the smallness of the impurity potential and gives reliable results in the Hermitian case [1,2,40]. So, what goes wrong in the bosonization procedure? The answer can be found by computing the single-particle spectrum of the Hamiltonian K. As shown in the inset of Fig. 3 (for more details, see [58]), we find that the imaginary part of the eigenvalues (i.e., the decay rates of the eigenstates) is mostly flat near the middle of the band (momentum close to $\pi/2$), while it has two peaks near the band edges. This contrasts with the bosonized Hamiltonian, which predicts the same decay rate for all states [90]. Therefore, bosonization is capable of describing the physics around the Fermi surface as long as the latter lies near the middle of the band (and this explains why it predicts the OC behavior correctly), but it cannot account for the nontrivial dynamics that occurs at the edges of the band. Indeed, this picture is confirmed by the time evolution of the occupation number of the momentum modes, shown in Fig. 3; while the discontinuity of the Fermi surface remains intact, the decay peaks cause an extra depletion deep inside the Fermi sea. Moreover, it can be observed that the depletion of these modes is more pronounced for smaller densities, in agreement with the increasing deviation of the dynamics from the predictions of bosonization in that regime. The breakdown of bosonization that we are proposing is unusual, since it does not come from properties of the band dispersion (such as the curvature at the Fermi surface [34]), but rather it comes from the properties of the imaginary part of the spectrum—the eigenstates' lifetimes.

The existence of this faster-decaying mode has been already noticed in Ref. [56], in which they appear as the ones most strongly scattered by the imaginary potential. The momenta at which the peaks occur are $\pm q^*$ and $\pm(\pi - q^*)$, where q^* is determined approximately [56] from the requirement that the group velocity of the fermions is equal to the strength of the imaginary potential, $2J \sin q^* = \gamma/2$. This observation implies that these special modes are a consequence of the curvature of the band dispersion. Indeed, if we start with a perfectly linear fermion dispersion, these modes disappear, and we find again that the various observables are in excellent agreement with the results from bosonization. Thus, the breakdown of bosonization at low densities is a curvature effect, albeit different from the usual beyond-TLL physics [34], since the latter involves only the curvature near the Fermi surface, whereas here we observe effects coming from the curvature at the band edges.

The observed decay properties within the Fermi surface explain why the system absorbs energy: the conservation of the number of particles implies that the fermions depleted from the low-momentum (and low-energy) special modes must populate higher-momentum states. The behavior of the return amplitude bears a similarity with the Hermitian OC in the presence of a bound state, where a nonanalytic dependence of $\mathcal{L}(t)$ on the density is found [91]—indeed, the special modes are quasibound states [92]. A direct generalization [58] of the Hermitian OC results from Ref. [50] to the present model allows us to have an analytical understanding on how the density influences the unrenormalized return amplitude $\tilde{\mathcal{L}}(t) \equiv \langle FS|\tilde{\psi}(t)\rangle = \langle FS|\, \mathrm{e}^{-\mathrm{i}Kt}\, |FS\rangle$. This calculation clearly shows how the imaginary potential causes $\tilde{\mathcal{L}}(t)$ to acquire an exponential decay that depends on the properties of all occupied states and is therefore nonuniversal and density dependent. We infer again that any bosonized version of the model that focuses on the states around the Fermi surface only can not possibly capture this nonuniversal decay.

Conclusions. From a fundamental point of view, our research unveils a mechanism for departures from bosonization that is distinct from more traditional explanations, rooted in the effects of band curvature of the dispersion relation [34]. In this regard, our findings illustrate transparently the profound difference between unitary and dissipative systems when it comes to the breakdown of low-energy collective descriptions.

Upon initial examination [58], the Lindblad dynamics governed by localized noise dephasing, albeit featuring the same

non-Hermitian Hamiltonian as this work, does not exhibit the same characteristic signatures of the measurement-induced dynamics that we found. This observation implies that quantum jumps may obscure the mechanism we have elucidated above. Unraveling these features and developing a simplified model for controlled breakdown of bosonization within Lindblad dynamics would represent a natural extension of our research.

Recently, measurement-induced phase transitions in low-dimensional fermionic systems have been captured using an effective bosonized description [26]. Our findings could serve as a promising starting point for extending this analysis to interacting fermions or quantum spin chains undergoing monitored dynamics. At variance with [26], one could wonder whether the universality classes of such dynamical transitions may change when the Tomonaga-Luttinger liquid description becomes inapplicable and processes similar to those presented here come into play. Among all the possible ramifications of our work, this appears to us as one of the most promising.

Acknowledgments. We wish to thank Z. Weinstein and S. Diehl for fruitful discussions and for providing comments on early versions of the manuscript. We also acknowledge the valuable observations provided by V. Meden. M.S. is grateful to R.J. Valencia Tortora and especially to O. Chelpanova for many useful discussions. This work has been supported by the Deutsche Forschungsgemeinschaft (DFG) through the Grant HADEQUAM-MA7003/3-1. We gratefully acknowledge the computing time granted through the project DysQCorr on the Mogon II supercomputer of the Johannes Gutenberg University Mainz [94], which is a member of the AHRP (Alliance for High Performance Computing in Rhineland Palatinate [95]), and the Gauss Alliance e.V.

[1] T. Giamarchi, *Quantum Physics in One Dimension*, 1st ed. (Clarendon Press, Oxford, 2003).
[2] A. O. Gogolin, A. A. Nersesyan, and A. M. Tsvelik, *Bosonization and Strongly Correlated Systems* (Cambridge University Press, Cambridge, 1998).
[3] M. A. Cazalilla, Effect of suddenly turning on interactions in the Luttinger model, Phys. Rev. Lett. **97**, 156403 (2006).
[4] A. Iucci and M. A. Cazalilla, Quantum quench dynamics of the Luttinger model, Phys. Rev. A **80**, 063619 (2009).
[5] M. A. Cazalilla and M.-C. Chung, Quantum quenches in the Luttinger model and its close relatives, J. Stat. Mech. (2016) 064004.
[6] J. Dziarmaga and M. Tylutki, Excitation energy after a smooth quench in a Luttinger liquid, Phys. Rev. B **84**, 214522 (2011).
[7] S. Ngo Dinh, D. A. Bagrets, and A. D. Mirlin, Interaction quench in nonequilibrium Luttinger liquids, Phys. Rev. B **88**, 245405 (2013).
[8] A. Iucci and M. A. Cazalilla, Quantum quench dynamics of the sine-Gordon model in some solvable limits, New J. Phys. **12**, 055019 (2010).
[9] M. Buchhold, M. Heyl, and S. Diehl, Prethermalization and thermalization of a quenched interacting Luttinger liquid, Phys. Rev. A **94**, 013601 (2016).
[10] E. Coira, F. Becca, and A. Parola, Quantum quenches in one-dimensional gapless systems, Eur. Phys. J. B **86**, 55 (2013).
[11] S. Porta, F. M. Gambetta, F. Cavaliere, N. T. Ziani, and M. Sassetti, Out-of-equilibrium density dynamics of a quenched fermionic system, Phys. Rev. B **94**, 085122 (2016).
[12] A. Bácsi and B. Dóra, Lindbladian route towards thermalization of a Luttinger liquid, Phys. Rev. B **107**, 125149 (2023).
[13] A. Bácsi, C. P. Moca, and B. Dóra, Dissipation-induced Luttinger liquid correlations in a one-dimensional Fermi gas, Phys. Rev. Lett. **124**, 136401 (2020).
[14] M. Buchhold and S. Diehl, Nonequilibrium universality in the heating dynamics of interacting Luttinger liquids, Phys. Rev. A **92**, 013603 (2015).
[15] H. Fröml, C. Muckel, C. Kollath, A. Chiocchetta, and S. Diehl, Ultracold quantum wires with localized losses: Many-body quantum Zeno effect, Phys. Rev. B **101**, 144301 (2020).
[16] A. Bácsi, C. P. Moca, G. Zaránd, and B. Dóra, Vaporization dynamics of a dissipative quantum liquid, Phys. Rev. Lett. **125**, 266803 (2020).
[17] I. Affleck, W. Hofstetter, D. R. Nelson, and U. Schollwöck, Non-Hermitian Luttinger liquids and flux line pinning in planar superconductors, J. Stat. Mech. (2004) P10003.
[18] Y. Ashida, S. Furukawa, and M. Ueda, Quantum critical behavior influenced by measurement backaction in ultracold gases, Phys. Rev. A **94**, 053615 (2016).
[19] B. Dóra and C. P. Moca, Quantum quench in $\mathcal{PT}$-symmetric luttinger liquid, Phys. Rev. Lett. **124**, 136802 (2020).
[20] Y. Ashida, S. Furukawa, and M. Ueda, Parity-time-symmetric quantum critical phenomena, Nat. Commun. **8**, 15791 (2017).
[21] B. Dóra and C. P. Moca, Full counting statistics in the many-body Hatano-Nelson model, Phys. Rev. B **106**, 235125 (2022).
[22] K. Yamamoto and N. Kawakami, Universal description of dissipative Tomonaga-Luttinger liquids with SU(N) spin symmetry: Exact spectrum and critical exponents, Phys. Rev. B **107**, 045110 (2023).
[23] B. Dóra, M. A. Werner, and C. P. Moca, Quantum quench dynamics in the Luttinger liquid phase of the Hatano-Nelson model, Phys. Rev. B **108**, 035104 (2023).
[24] A. Dubey, S. Biswas, and A. Kundu, Operator correlations in a quenched non-Hermitian Luttinger liquid, Phys. Rev. B **108**, 085433 (2023).
[25] S. J. Garratt, Z. Weinstein, and E. Altman, Measurements conspire nonlocally to restructure critical quantum states, Phys. Rev. X **13**, 021026 (2023).
[26] M. Buchhold, Y. Minoguchi, A. Altland, and S. Diehl, Effective theory for the measurement-induced phase transition of Dirac fermions, Phys. Rev. X **11**, 041004 (2021).
[27] B. Ladewig, S. Diehl, and M. Buchhold, Monitored open fermion dynamics: Exploring the interplay of measurement, decoherence, and free Hamiltonian evolution, Phys. Rev. Res. **4**, 033001 (2022).
[28] K. Yamamoto, M. Nakagawa, M. Tezuka, M. Ueda, and N. Kawakami, Universal properties of dissipative Tomonaga-Luttinger liquids: Case study of a non-Hermitian XXZ spin chain, Phys. Rev. B **105**, 205125 (2022).

[29] X. Sun, H. Yao, and S.-K. Jian, New critical states induced by measurement, arXiv:2301.11337.
[30] M. Collura, P. Calabrese, and F. H. L. Essler, Quantum quench within the gapless phase of the spin $-\frac{1}{2}$ Heisenberg XXZ spin chain, Phys. Rev. B **92**, 125131 (2015).
[31] F. Pollmann, M. Haque, and B. Dóra, Linear quantum quench in the Heisenberg XXZ chain: Time-dependent Luttinger-model description of a lattice system, Phys. Rev. B **87**, 041109(R) (2013).
[32] C. Karrasch, J. Rentrop, D. Schuricht, and V. Meden, Luttinger-liquid universality in the time evolution after an interaction quench, Phys. Rev. Lett. **109**, 126406 (2012).
[33] D. M. Kennes and V. Meden, Luttinger liquid properties of the steady state after a quantum quench, Phys. Rev. B **88**, 165131 (2013).
[34] A. Imambekov, T. L. Schmidt, and L. I. Glazman, One-dimensional quantum liquids: Beyond the Luttinger liquid paradigm, Rev. Mod. Phys. **84**, 1253 (2012).
[35] D. B. Gutman, Y. Gefen, and A. D. Mirlin, Nonequilibrium Luttinger liquid: Zero-bias anomaly and dephasing, Phys. Rev. Lett. **101**, 126802 (2008).
[36] D. B. Gutman, Y. Gefen, and A. D. Mirlin, Bosonization of one-dimensional fermions out of equilibrium, Phys. Rev. B **81**, 085436 (2010).
[37] D. B. Gutman, Y. Gefen, and A. D. Mirlin, Full counting statistics of a Luttinger liquid conductor, Phys. Rev. Lett. **105**, 256802 (2010).
[38] P. W. Anderson, Infrared catastrophe in Fermi gases with local scattering potentials, Phys. Rev. Lett. **18**, 1049 (1967).
[39] G. D. Mahan, *Many-Particle Physics*, 2nd ed. (Plenum Press, New York, 1993).
[40] K. D. Schotte and U. Schotte, Tomonaga's model and the threshold singularity of x-ray spectra of metals, Phys. Rev. **182**, 479 (1969).
[41] A. C. Hewson, *The Kondo Problem to Heavy Fermions*, Cambridge Studies in Magnetism (Cambridge University Press, Cambridge, 1993).
[42] P. Coleman, New approach to the mixed-valence problem, Phys. Rev. B **29**, 3035 (1984).
[43] G. Yuval and P. W. Anderson, Exact results for the Kondo problem: One-body theory and extension to finite temperature, Phys. Rev. B **1**, 1522 (1970).
[44] M. Heyl and S. Kehrein, X-ray edge singularity in optical spectra of quantum dots, Phys. Rev. B **85**, 155413 (2012).
[45] N. d'Ambrumenil and B. Muzykantskii, Fermi gas response to time-dependent perturbations, Phys. Rev. B **71**, 045326 (2005).
[46] F. Grusdt, K. Seetharam, Y. Shchadilova, and E. Demler, Strong-coupling Bose polarons out of equilibrium: Dynamical renormalization-group approach, Phys. Rev. A **97**, 033612 (2018).
[47] M. Knap, A. Shashi, Y. Nishida, A. Imambekov, D. A. Abanin, and E. Demler, Time-dependent impurity in ultracold fermions: Orthogonality catastrophe and beyond, Phys. Rev. X **2**, 041020 (2012).
[48] A. Shashi, F. Grusdt, D. A. Abanin, and E. Demler, Radio-frequency spectroscopy of polarons in ultracold Bose gases, Phys. Rev. A **89**, 053617 (2014).
[49] P. Nozières and C. T. De Dominicis, Singularities in the x-ray absorption and emission of metals. III. One-body theory exact solution, Phys. Rev. **178**, 1097 (1969).
[50] M. Combescot and P. Nozières, Infrared catastrophy and excitons in the x-ray spectra of metals, J. Phys. (France) **32**, 913 (1971).
[51] F. Tonielli, R. Fazio, S. Diehl, and J. Marino, Orthogonality catastrophe in dissipative quantum many-body systems, Phys. Rev. Lett. **122**, 040604 (2019).
[52] C. Lupo and M. Schiró, Transient Loschmidt echo in quenched Ising chains, Phys. Rev. B **94**, 014310 (2016).
[53] M. Schiró and A. Mitra, Transient orthogonality catastrophe in a time-dependent nonequilibrium environment, Phys. Rev. Lett. **112**, 246401 (2014).
[54] W. Berdanier, J. Marino, and E. Altman, Universal dynamics of stochastically driven quantum impurities, Phys. Rev. Lett. **123**, 230604 (2019).
[55] C. Jung, M. Müller, and I. Rotter, Phase transitions in open quantum systems, Phys. Rev. E **60**, 114 (1999).
[56] P. C. Burke, J. Wiersig, and M. Haque, Non-Hermitian scattering on a tight-binding lattice, Phys. Rev. A **102**, 012212 (2020).
[57] L. Rosso, F. Iemini, M. Schirò, and L. Mazza, Dissipative flow equations, SciPost Phys. **9**, 091 (2020).
[58] See Supplemental Material at http://link.aps.org/supplemental/10.1103/PhysRevResearch.6.L042022 for more analytical details and additional numerical results.
[59] H. M. Wiseman and G. J. Milburn, *Quantum Measurement and Control* (Cambridge University Press, Cambridge, 2009).
[60] M. A. Nielsen and I. L. Chuang, *Quantum Computation and Quantum Information: 10th Anniversary Edition* (Cambridge University Press, Cambridge, 2010).
[61] X. Turkeshi and M. Schiró, Entanglement and correlation spreading in non-Hermitian spin chains, Phys. Rev. B **107**, L020403 (2023).
[62] Y. Le Gal, X. Turkeshi, and M. Schirò, Volume-to-area law entanglement transition in a non-Hermitian free fermionic chain, SciPost Phys. **14**, 138 (2023).
[63] X. Turkeshi, A. Biella, R. Fazio, M. Dalmonte, and M. Schiró, Measurement-induced entanglement transitions in the quantum Ising chain: From infinite to zero clicks, Phys. Rev. B **103**, 224210 (2021).
[64] A. J. Daley, Quantum trajectories and open many-body quantum systems, Adv. Phys. **63**, 77 (2014).
[65] Up to a constant shift $K - \tilde{H} \propto \mathbb{1}$.
[66] M. Foss-Feig, A. J. Daley, J. K. Thompson, and A. M. Rey, Steady-state many-body entanglement of hot reactive fermions, Phys. Rev. Lett. **109**, 230501 (2012).
[67] M. Naghiloo, M. Abbasi, Y. N. Joglekar, and K. W. Murch, Quantum state tomography across the exceptional point in a single dissipative qubit, Nat. Phys. **15**, 1232 (2019).
[68] H. F. Fröml, Localized dissipation in fermionic quantum wires, Ph.D. thesis, Universität zu Köln, 2020.
[69] H. Fröml, A. Chiocchetta, C. Kollath, and S. Diehl, Fluctuation-induced quantum Zeno effect, Phys. Rev. Lett. **122**, 040402 (2019).
[70] T. Müller, M. Gievers, H. Fröml, S. Diehl, and A. Chiocchetta, Shape effects of localized losses in quantum wires: Dissipative resonances and nonequilibrium universality, Phys. Rev. B **104**, 155431 (2021).
[71] P. L. Krapivsky, K. Mallick, and D. Sels, Free fermions with a localized source, J. Stat. Mech. (2019) 113108.

[72] P. E. Dolgirev, J. Marino, D. Sels, and E. Demler, Non-Gaussian correlations imprinted by local dephasing in fermionic wires, Phys. Rev. B **102**, 100301(R) (2020).

[73] Y. Takasu, T. Yagami, Y. Ashida, R. Hamazaki, Y. Kuno, and Y. Takahashi, PT-symmetric non-Hermitian quantum many-body system using ultracold atoms in an optical lattice with controlled dissipation, Prog. Theor. Exp. Phys. **2020**, 12A110 (2020).

[74] S. Krinner, T. Esslinger, and J.-P. Brantut, Two-terminal transport measurements with cold atoms, J. Phys.: Condens. Matter **29**, 343003 (2017).

[75] M. Lebrat, S. Häusler, P. Fabritius, D. Husmann, L. Corman, and T. Esslinger, Quantized conductance through a spin-selective atomic point contact, Phys. Rev. Lett. **123**, 193605 (2019).

[76] M.-Z. Huang, J. Mohan, A.-M. Visuri, P. Fabritius, M. Talebi, S. Wili, S. Uchino, T. Giamarchi, and T. Esslinger, Superfluid signatures in a dissipative quantum point contact, Phys. Rev. Lett. **130**, 200404 (2023).

[77] M. Lebrat, P. Grišins, D. Husmann, S. Häusler, L. Corman, T. Giamarchi, J.-P. Brantut, and T. Esslinger, Band and correlated insulators of cold fermions in a mesoscopic lattice, Phys. Rev. X **8**, 011053 (2018).

[78] L. Corman, P. Fabritius, S. Häusler, J. Mohan, L. H. Dogra, D. Husmann, M. Lebrat, and T. Esslinger, Quantized conductance through a dissipative atomic point contact, Phys. Rev. A **100**, 053605 (2019).

[79] B. Yan, S. A. Moses, B. Gadway, J. P. Covey, K. R. A. Hazzard, A. M. Rey, D. S. Jin, and J. Ye, Observation of dipolar spin-exchange interactions with lattice-confined polar molecules, Nature (London) **501**, 521 (2013).

[80] B. Zhu, B. Gadway, M. Foss-Feig, J. Schachenmayer, M. L. Wall, K. R. A. Hazzard, B. Yan, S. A. Moses, J. P. Covey, D. S. Jin, J. Ye, M. Holland, and A. M. Rey, Suppressing the loss of ultracold molecules via the continuous quantum Zeno effect, Phys. Rev. Lett. **112**, 070404 (2014).

[81] K. Sponselee, L. Freystatzky, B. Abeln, M. Diem, B. Hundt, A. Kochanke, T. Ponath, B. Santra, L. Mathey, K. Sengstock, and C. Becker, Dynamics of ultracold quantum gases in the dissipative Fermi–Hubbard model, Quantum Sci. Technol. **4**, 014002 (2018).

[82] K. Honda, S. Taie, Y. Takasu, N. Nishizawa, M. Nakagawa, and Y. Takahashi, Observation of the sign reversal of the magnetic correlation in a driven-dissipative Fermi gas in double wells, Phys. Rev. Lett. **130**, 063001 (2023).

[83] T. Tomita, S. Nakajima, Y. Takasu, and Y. Takahashi, Dissipative Bose-Hubbard system with intrinsic two-body loss, Phys. Rev. A **99**, 031601 (2019).

[84] N. Syassen, D. M. Bauer, M. Lettner, T. Volz, D. Dietze, J. J. García-Ripoll, J. I. Cirac, G. Rempe, and S. Dürr, Strong dissipation inhibits losses and induces correlations in cold molecular gases, Science **320**, 1329 (2008).

[85] M. Cetina, M. Jag, R. S. Lous, I. Fritsche, J. T. M. Walraven, R. Grimm, J. Levinsen, M. M. Parish, R. Schmidt, M. Knap, and E. Demler, Ultrafast many-body interferometry of impurities coupled to a Fermi sea, Science **354**, 96 (2016).

[86] X. Cao, A. Tilloy, and A. D. Luca, Entanglement in a fermion chain under continuous monitoring, SciPost Phys. **7**, 024 (2019).

[87] The disagreement of the fitted exponent with respect to β_b at larger γ can be attributed to the local curvature of the dispersion around the Fermi energy, just as in the Hermitian case [1,2].

[88] Unless the density is too low or too high, so that the Fermi momentum crosses the special momenta q^* reported in the following section. There are also qualitative changes in the nonperturbative regime $\gamma > 4J$ caused by the crossing of an exceptional point [56,68], not treated here.

[89] C. L. Kane, K. A. Matveev, and L. I. Glazman, Fermi-edge singularities and backscattering in a weakly interacting one-dimensional electron gas, Phys. Rev. B **49**, 2253 (1994).

[90] Indeed, it differs from a $\mathcal{PT}$-symmetric [93] Hamiltonian by an imaginary constant only, which is unobservable in the nonlinear dynamics Eq. (1).

[91] A. M. Zagoskin and I. Affleck, Fermi edge singularities: Bound states and finite-size effects, J. Phys. A: Math. Gen. **30**, 5743 (1997).

[92] X. Xie, G. Liang, F. Ma, Y. Du, Y. Peng, E. Li, H. Chen, L. Li, F. Gao, and H. Xue, Observation of scale-free localized states induced by non-Hermitian defects, Phys. Rev. B **109**, L140102 (2024).

[93] Y. Ashida, Z. Gong, and M. Ueda, Non-Hermitian physics, Adv. Phys. **69**, 249 (2020).

[94] https://hpc.uni-mainz.de/

[95] www.ahrp.info